Electron-impact ionization of atoms in high-temperature dense plasmas

M. S. Pindzola and S. D. Loch
Department of Physics, Auburn University, Auburn 36849, Alabama, USA

J. Colgan and C. J. Fontes
Los Alamos National Laboratory, Los Alamos 87545, New Mexico, USA

(Received 14 March 2008; published 16 June 2008)

Electron-impact ionization cross sections for atoms in high-temperature dense plasmas are calculated in a configuration-average distorted-wave method. For those conditions in which the Coulomb coupling parameter is small, we use the Debye-Hückel potential to screen the projectile electron from the nucleus and target electrons. Ionization cross sections are calculated for both Ne^{4+} and Au^{47+} at high temperatures and various electron densities up to 1.0×10^{25} cm^{-3}. In general we find that as the density increases, the ionization cross section decreases at all incident energies. We also find that as the charge on the atomic ion becomes larger, the relative density effect becomes smaller.

DOI: 10.1103/PhysRevA.77.062707 PACS number(s): 34.50.Fa

I. INTRODUCTION

The radiative properties of high-temperature dense plasmas, such as those found in inertial confinement fusion devices, x-ray lasers, and various astrophysical objects, remain a subject of current interest [1]. Since most hot dense laboratory plasmas are not in local thermodynamic equilibrium, it is important to understand how the various electron-ion collision processes that determine ion stage abundance and radiative power loss are modified by plasma effects. For weakly coupled plasmas, in which a Coulomb coupling parameter Γ defined in terms of the ratio of the average potential to kinetic energy for a given ion stage is less than one, various projectile-target electron screening methods have been shown to be useful [2].

In this paper, we examine the influence of a weakly coupled high temperature dense plasma on the electron-impact ionization of atomic ions. We choose densities high enough to influence the projectile-ion interaction, but not high enough to affect the target electrons of the atomic ion. For simplicity, we choose the Debye-Hückel screening model [3], as applied to study hot dense plasma effects on the electron-impact excitation of atomic ions in the classic paper of Whitten, Lane, and Weisheit [4]. In recent years, the influence of hot dense plasma effects on the electron-impact excitation [5] and ionization [6] of Au atomic ions has been studied using various other plasma screening models.

The rest of the paper is structured as follows. Section II describes our incorporation of the Debye-Hückel screening model into a configuration-average distorted-wave method for the electron-impact ionization of atomic ions, Sec. III presents cross section results for the $2p$ subshell ionization of Ne^{4+} and the $4p$ subshell ionization of Au^{47+} at various electron temperatures and densities, and Sec. IV concludes with a brief summary and future plans. Unless otherwise stated, we will use atomic units.

II. THEORY

For direct ionization, a general transition between configurations has the form

$$(nl)^w k_i l_i \rightarrow (nl)^{w-1} k_e l_e k_f l_f, \tag{1}$$

where w is a subshell occupation number, nl are quantum numbers of the bound electron, and $k_i l_i$, $k_e l_e$, $k_f l_f$ are quantum numbers of the initial, ejected, and final continuum electrons. The configuration-average direct ionization cross section is given by [7]

$$\sigma = \int_0^{E/2} d\epsilon_e \frac{32w}{k_i^3 k_e k_f} \sum_{l_i} \sum_{l_f} \sum_{l_e} (2l_i+1)(2l_f+1) \times (2l_e+1) S(k_e l_e, k_f l_f, nl, k_i l_i), \tag{2}$$

where $E=(k_e^2+k_f^2)/2$. A configuration-average over the scattering matrix squared yields

$$S(k_e l_e, k_f l_f, nl, k_i l_i) = \sum_{\lambda} \begin{pmatrix} l_e & \lambda & l \\ 0 & 0 & 0 \end{pmatrix}^2 \begin{pmatrix} l_i & \lambda & l_f \\ 0 & 0 & 0 \end{pmatrix}^2 \frac{[R^{\lambda}(k_e l_e, k_f l_f, nl, k_i l_i)]^2}{(2\lambda+1)} + \sum_{\lambda'} \begin{pmatrix} l_e & \lambda' & l_i \\ 0 & 0 & 0 \end{pmatrix}^2 \begin{pmatrix} l & \lambda' & l_f \\ 0 & 0 & 0 \end{pmatrix}^2 \frac{[R^{\lambda'}(k_f l_f, k_e l_e, nl, k_i l_i)]^2}{(2\lambda'+1)}$$
$$- \sum_{\lambda} \sum_{\lambda'} (-1)^{\lambda+\lambda'} \begin{pmatrix} l_e & \lambda & l \\ 0 & 0 & 0 \end{pmatrix} \begin{pmatrix} l_i & \lambda & l_f \\ 0 & 0 & 0 \end{pmatrix} \begin{pmatrix} l_e & \lambda' & l_i \\ 0 & 0 & 0 \end{pmatrix} \begin{pmatrix} l & \lambda' & l_f \\ 0 & 0 & 0 \end{pmatrix}$$
$$\times \begin{Bmatrix} l_e & l & \lambda \\ l_f & l_i & \lambda' \end{Bmatrix} R^{\lambda}(k_e l_e, k_f l_f, nl, k_i l_i) R^{\lambda'}(k_f l_f, k_e l_e, nl, k_i l_i), \tag{3}$$

where the angular coefficients are expressed in terms of standard 3-j and 6-j symbols.

The Coulomb radial matrix element is given by

$$R^{\lambda}(k_e l_e, k_f l_f, nl, k_i l_i) = \int_0^{\infty} dr_1 \int_0^{\infty} dr_2 \frac{r_<^{\lambda}}{r_>^{\lambda+1}} e^{-r_2/\Lambda} P_{k_e l_e}(r_1) P_{k_f l_f}(r_2) P_{nl}(r_1) P_{k_i l_i}(r_2), \quad (4)$$

where $r_<=\min(r_1,r_2)$ and $r_>=\max(r_1,r_2)$. The Debye-Hückel screening radius is given by

$$\Lambda = \sqrt{\frac{T_e}{4\pi N_e}}, \quad (5)$$

where T_e is the electron temperature (1 a.u.=27.212 eV) and N_e is the electron density (1 a.u.=6.75×10^{24} cm^{-3}). For our choice of densities high enough to influence the projectile-ion interaction, but not high enough to affect the target electrons, the exponential screening factor in Eq. (4) only includes the projectile radius r_2.

The energies and bound orbitals needed to evaluate the configuration-average direct ionization cross section are calculated in the Hartree-Fock relativistic (HFR) approximation [8], which includes mass-velocity and Darwin corrections. The ejected electron distorted-wave orbitals are found by solving a single-channel radial Schrödinger equation given by

$$\left(-\frac{1}{2}\frac{d^2}{dr^2} + \frac{l(l+1)}{2r^2} - \frac{Z}{r} + V_{\mathrm{HXR}}^{N-1}(r)\right) P_{kl}(r) = \frac{k^2}{2} P_{kl}(r), \quad (6)$$

where Z is the nuclear charge and $V_{\mathrm{HXR}}^{N-1}(r)$ is an $(N-1)$ electron Hartree with local exchange potential, which also includes mass-velocity and Darwin corrections. The initial and final electron distorted-wave orbitals are found by solving a single-channel radial Schrödinger equation given by

$$\left(-\frac{1}{2}\frac{d^2}{dr^2} + \frac{l(l+1)}{2r^2} - \frac{Z}{r}e^{-r/\Lambda} + V_{\mathrm{HXR}}^{N}(r)e^{-r/\Lambda}\right) P_{kl}(r) = \frac{k^2}{2} P_{kl}(r), \quad (7)$$

where $V_{\mathrm{HXR}}^{N}(r)$ is an N electron Hartree with local exchange potential and relativistic corrections. Again in keeping with our choice of density range, an exponential screening factor modifies the potential terms for the scattered electron distorted waves of Eq. (7), but not the potential terms for the ejected electron distorted waves of Eq. (6).

III. RESULTS

As a check on our numerical methods, we first calculated the electron-impact excitation cross section for the $1s\rightarrow2p$ transition in Ne^{9+} to compare with the three state close-coupling results of Whitten, Lane, and Weisheit [4]. The configuration-average excitation cross section is given by [7]

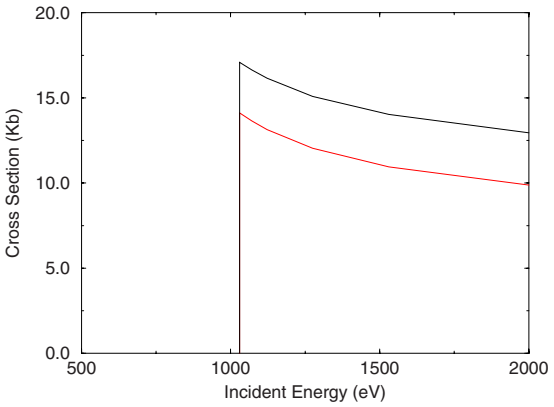

FIG. 1. (Color online) Electron-impact excitation of Ne^{9+}. Black (upper) line: baseline DW calculation, red (lower) line: DW calculation at T_e=500 eV and $N_e=1.1\times10^{24}$ cm^{-3} (1.0 kb=1.0×10^{-21} cm^2).

$$\sigma = \frac{48\pi}{k_i^3 k_f} \sum_{l_i} \sum_{l_f} (2l_i+1)(2l_f+1) S(2p, k_f l_f, 1s, k_i l_i), \quad (8)$$

where the scattering matrix squared is given by Eqs. (3) and (4), while the initial and final electron distorted-waves are calculated using Eq. (7). For the choice of $N_e=1.1\times10^{24}$ cm^{-3} and T_e=500 eV, the Coulomb coupling parameter $\Gamma=0.43$, the mean radii of the excited orbitals are $\langle r\rangle_{1s}=0.15$ and $\langle r\rangle_{2p}=0.50$, and the Debye-Hückel screening radius is $\Lambda=3.0$. As shown in Fig. 1, the high-temperature dense plasma $1s\rightarrow2p$ cross section is about 20% lower than the baseline $1s\rightarrow2p$ cross section for Ne^{9+}. Furthermore, the configuration-average distorted-wave results for both excitation cross sections are in very good agreement with the three state close-coupling results of Whitten, Lane, and Weisheit [4], as found in Fig. 3(b) of their paper.

We then calculated the electron-impact ionization cross section for the outer subshell of $Ne^{4+}(1s^2 2s^2 2p^2)$. The plasma parameters for the Ne^{4+} ionization calculations are given in Table I. For electron densities less than 1.0×10^{24} cm^{-3} and T_e=500 eV, the Coulomb coupling parameter is much less than 1.0. The Debye-Hückel screening radius is found to be much larger than the mean radius of the $2p$ orbital, validating that the plasma for these densities has only a small effect on the bound orbitals. As shown in Fig. 2, the $2p$ ionization cross section for Ne^{4+} decreases at all incident energies as the electron density is increased. At around 300 eV incident energy, the $N_e=1.0\times10^{24}$ cm^{-3} ionization cross section is about 50% lower than the baseline cross section. We note that the total ionization cross section for Ne^{4+} should include contributions from the direct ionization of the $2s$ subshell, with an ionization potential of 143 eV and a peak baseline cross section of about 1.3 Mb. Further calculations at temperatures T_e=125 eV near the ionization potential of Ne^{4+} also show a decrease in the $2p$ ionization cross section as a function of density, although the coupling parameter Γ increases by a factor of 4 and is just below one for the higher densities.

Finally, we calculated the electron-impact ionization cross section for the outer subshell of

TABLE I. Plasma parameters for ionization calculations. Electron temperature T_e, electron density N_e, mean radius of ionized orbital $\langle r \rangle$ in a.u., Coulomb coupling parameter Γ, Debye-Hückel screening radius Λ in a.u.

Atomic ion	T_e (eV)	N_e (cm^{-3})	$\langle r \rangle$	Γ	Λ
Ne^{4+}	500	1.0×10^{22}	0.70	0.04	31.4
		1.0×10^{23}		0.09	9.9
		1.0×10^{24}		0.18	3.1
Au^{47+}	10000	1.0×10^{23}	0.37	0.05	44.4
		1.0×10^{24}		0.11	14.1
		1.0×10^{25}		0.23	4.4

$Au^{47+}(1s^22s^22p^63s^23p^63d^{10}4s^24p^2)$ to better understand how density effects scale with the charge on the atomic ion. The plasma parameters for the Au^{47+} ionization calculations are given in Table I. For electron densities less than 1.0×10^{25} cm^{-3} and $T_e=10\,000$ eV, the Coulomb coupling parameter is much less than 1.0. The Debye-Hückel screening radius is found to be much larger than the mean radius of the $4p$ orbital. As shown in Fig. 3, the $4p$ ionization cross section for Au^{47+} decreases at all incident energies as the electron density is increased. At around 6000 eV incident energy, the $N_e=1.0\times10^{25}$ cm^{-3} ionization cross section is about 20% lower than the baseline cross section. We note that the total ionization cross section for Au^{47+} is dominated by contributions from the direct ionization of the $3d$ subshell, with an ionization potential of 4600 eV and a peak baseline cross section of about 10 kb. Additional contributions are made from the direct ionization of the $4s$ subshell, with an ionization potential of 2760 eV and a peak baseline cross section of about 3.7 kb, and from $3d\rightarrow5l$ excitations leading to autoionization. Further calculations at temperatures $T_e=2500$ eV near the ionization potential of Au^{47+} also show a decrease in the $4p$ ionization cross section as a function of density, although the coupling parameter Γ increases by a factor of 4 and is just below one for the higher densities.

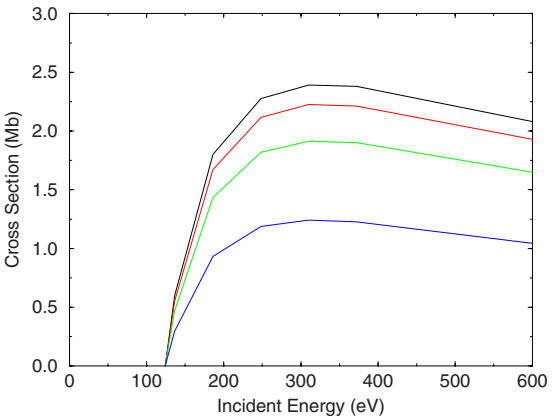

FIG. 2. (Color online) Electron-impact ionization of Ne^{4+}. Black (topmost) line: baseline DW calculation, red (second from top) line: DW calculation at $T_e=500$ eV and $N_e=1.0\times10^{22}$ cm^{-3}, green (third from top) line: DW calculation at $T_e=500$ eV and $N_e=1.0\times10^{23}$ cm^{-3}, blue (bottommost) line: DW calculation at $T_e=500$ eV and $N_e=1.0\times10^{24}$ cm^{-3} (1.0 kb$=1.0\times10^{-18}$ cm^2).

Our choice of Au^{47+} was also based on being able to compare our results with the ion-sphere model distorted-wave calculations of Wu *et al.* [6]. Although our configuration-average distorted-wave baseline cross sections for the $2p$ ionization of $Ge^{22+}(1s^22s^22p^6)$ are in very good agreement with the distorted-wave results of Wu *et al.* [6], as found in Fig. 1 of their paper, our configuration-average distorted-wave baseline cross sections for the $4p$ ionization of Au^{47+} are a factor of 2 larger than their distorted-wave results, as found in Fig. 2 of their paper. We suspect that their baseline cross sections are missing a $w=2$ occupation number multiplication [see Eq. (2)], or that their cross sections are for the $4p$ ionization of Au^{48+}.

More importantly, the plasma effects included in the Wu *et al.* [6] calculations result in a cross section that increases at all incident energies as the electron density is increased, as found in Fig. 2 of their paper, which is completely opposite from our findings reported in Fig. 3. Since the Coulomb coupling parameter for their highest density case of 1.0 gm/cm^3 at $T_e=1000$ eV is still less than 1, and the corresponding Debye-Hückel screening radius of $\Lambda=12$ is much greater than the mean radius of the $4p$ orbital, our calculations for their precise parameters should be valid and yet show a decrease in the ionization cross section as the elec-

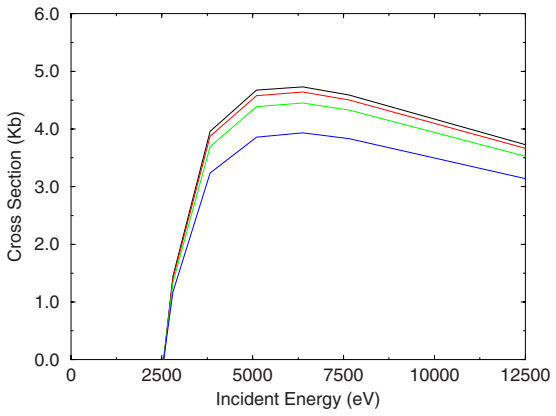

FIG. 3. (Color online) Electron-impact ionization of Au^{47+}. Black (topmost) line: baseline DW calculation, red (second from top) line: DW calculation at $T_e=10\,000$ eV and $N_e=1.0\times10^{23}$ cm^{-3}, green (third from top) line: DW calculation at $T_e=10\,000$ eV and $N_e=1.0\times10^{24}$ cm^{-3}, blue (bottommost) line: DW calculation at $T_e=10\,000$ eV and $N_e=1.0\times10^{25}$ cm^{-3} (1.0 kb$=1.0\times10^{-21}$ cm^2).

tron density increases. If we remove the exponential screening factor from the Coulomb matrix element of Eq. (4) and also place an exponential screening factor on the potential terms for the ejected electron distorted-waves in Eq. (6), our calculations for their precise parameters now show an increase in the ionization cross section as the electron density increases. However, we still feel that the choice made by Whitten *et al.* [4] to just screen the projectile electron is proper for those electron densities not yet strong enough to affect the core electrons of the target ion. We also note that both our calculations using the Wu *et al.* [6] temperature and densities parameters show substantially smaller density effects on the baseline cross section than those found in Fig. 2 of their paper.

IV. SUMMARY

A perturbative distorted-wave method has been modified to enable the calculation of electron-impact ionization cross sections for atomic ions embedded in hot dense plasmas. For weakly coupled plasmas and electron densities that do not disturb the target ion bound electrons, we find that outer subshell direct ionization cross sections are reduced for both Ne^{4+} and Au^{47+}, although the plasma effect reduction is not as large for the more highly charged species.

In the future, we plan to apply the configuration-average distorted-wave method with plasma screening effects to generate electron-ion collision data along an entire isonuclear sequence, for example Ne. Since the basic excitation, ionization, and recombination cross sections will now depend on temperature and density, the solution of the collisional-radiative equations for the excited states becomes more involved. However, once generalized collisional-radiative (GCR) coefficients [9] for ionization, recombination, and radiated power loss are in hand, further studies of ion-stage fractional abundances and total radiated power loss in hot dense plasmas proceeds in a manner similar to the studies done recently for relatively low temperature and density Li [10,11] and Ar [12] plasmas.

ACKNOWLEDGMENTS

This work was supported in part by grants from the U.S. Department of Energy. Computational work was carried out at the National Energy Research Scientific Computing Center in Oakland, California.

[1] "Radiative Properties of Hot Dense Matter", special issue of J. Quant. Spectrosc. Radiat. Transf. **99**, III (2006).
[2] M. S. Murillo and J. C. Weisheit, Phys. Rep. **302**, 1 (1998).
[3] P. Debye and E. Hückel, Z. Phys. **24**, 185 (1923).
[4] B. L. Whitten, N. F. Lane, and J. C. Weisheit, Phys. Rev. A **29**, 945 (1984).
[5] J. K. Yuan, Y. S. Sun, and S. T. Zheng, J. Phys. B **29**, 153 (1996).
[6] Z. Q. Wu, G. X. Han, J. Yan, and J. Q. Pang, J. Phys. B **35**, 2305 (2002).
[7] M. S. Pindzola, D. C. Griffin, and C. Bottcher, in *Atomic Processes in Electron-Ion and Ion-Ion Collisions*, Vol. 145 of *NATO Advanced Studies Institue, Series B: Physics* (Plenum, New York, 1986), p. 75.
[8] R. D. Cowan, *The Theory of Atomic Structure and Spectra* (University of California Press, Berkeley, 1981).
[9] S. D. Loch, S. A. Abdel-Naby, C. P. Ballance, and M. S. Pindzola, Phys. Rev. A **76**, 022706 (2007).
[10] H. P. Summers and M. G. O'Mullane, in *Nuclear Fusion Research*, edited by R. E. H. Clark and D. H. Reiter (Springer, Berlin, 2005), p. 399.
[11] S. D. Loch, C. J. Fontes, J. Colgan, M. S. Pindzola, C. P. Ballance, D. C. Griffin, M. G. O'Mullane, and H. P. Summers, Phys. Rev. E **69**, 066405 (2004).
[12] S. D. Loch, Sh. A. Abdel-Naby, C. P. Ballance, and M. S. Pindzola, Phys. Rev. A **76**, 022706 (2007).